BRAZILIAN JOURNAL OF OCEANOGRAPHY, 59(3):241-252, 2011

STUDY OF THE SURFACE WATER CIRCULATION IN SAN BLAS CHANNEL (ARGENTINA) USING LANDSAT IMAGERY

Débora Beigt[1], Diana G. Cuadrado[2,3] and María C. Piccolo[2,4]*

[1]Instituto de Investigaciones en Biodiversidad y Medioambiente (CONICET-UNCo)
(Quintral 1250, (8400) S.C. de Bariloche, Río Negro, Argentina)

[2]Instituto Argentino de Oceanografia (CONICET-UNS), Bahia Blanca, Argentina

[3]Departamento de Geología, Universidad Nacional del Sur, Bahia Blanca, Argentina

[4]Departamento de Geografía y Turismo, Universidad Nacional del Sur, Bahia Blanca, Argentina

*Corresponding autor: dbeigt@conicet.gov.ar

ABSTRACT

This paper deals with the application of satellite images to study turbidity and water circulation patterns in San Blas channel during a theoretical tidal cycle. Eight Landsat TM and ETM images acquired under clear-sky conditions and representing different tidal stages were selected from a pool of Landsat images provided by the argentinean National Commission of Space Activities (CONAE) and the US Geological Survey. Standard digital image processing techniques were used to perform geometric and radiometric corrections on the visible and near-infrared bands. An image-based atmospheric correction (COST method by CHAVEZ, 1996) was applied. An ISODATA unsupervised classification was performed in order to identify different turbidity levels throughout the channel and adjacent areas. The results suggest that suspended sediment transport towards the channel mouth by ebb currents occurs along both flanks. These currents carry suspended sediment into the open sea, generating an ebb tidal delta which tends to rotate in a clockwise direction. Flood currents trigger turbidity mostly over the southern flank of the channel, generating a flood tidal delta with elongated banks extending in the direction of the tidal currents. From the elongated shape of the turbidity plumes, general tidal circulation patterns were identified.

RESUMO

Este trabalho analisa a turbidez e a circulação da agua no canal San Blas durante um ciclo de maré teórico através de imagens satelitais. Foram utilizadas 8 imagens Landsat TM e ETM adquiridas em condições de céu claro e ao longo de diferentes momentos da maré. As imagens foram proporcionadas pela Comisión Nacional de Actividades Espaciales (CONAE) y pelo Serviço Geológico dos Estados Unidos (USGS). As correções geométricas e radiométricas foram realizadas nas bandas do espectro visível e do infravermelho próximo, utilizando técnicas padrões de processamento digital. Foi aplicada a correção atmosférica COST (CHAVEZ, 1996). Foi realizada uma classificação ISODATA não supervisionada para identificar diferentes níveis de turbidez al longo do canal e zonas adjacentes. Os resultados sugerem que o transporte de sedimento em suspensão para a boca do canal se da ao longo de ambos flancos, pela ação das correntes de refluxo. Estas correntes geram um delta de refluxo com uma tendência de rotação para a direção sul. As correntes de fluxo provocam turbidez principalmente sobre a costa sul do canal, gerando um delta de fluxo com bancos alargados na direção das correntes de maré. As plumas de turbidez permitiram identificar padrões gerais de circulação da maré.

Descriptors**:** Turbidity, Water circulation, Landsat imagery, San Blas channel.
Descritores: Turbidez, Circulação da água, Imagens Landsat, Canal San Blas.

INTRODUCTION

The San Blas channel (40º34´S, 62º11´W) is situated in the southern portion of Anegada bay, a large embayment covering 2371 km^2 on the Atlantic coast of Buenos Aires province, Argentina (Fig. 1). Anegada bay is an area of high ecological value in terms of marine biodiversity. Commercial, sporting

and artisanal fisheries have historically exploited the bay´s resources. In order to protect its fauna, a Nature Reserve was established in 1987, its status being changed to that of Multiple-Use Reserve in 2001. The San Blas channel connects the bay and the continental shelf. Thus, hydrographic studies focusing on its water circulation are important for a better understanding of the ecosystem´s dynamics, including the spatial distribution of the aquatic populations and the sediment transport processes.

In this paper, turbidity and water circulation patterns in San Blas channel are studied during a theoretical tidal cycle. BABAN (1995) refers to turbidity as the opaqueness of water, which may be caused by a wide range of factors such as suspended sediment concentrations, biological activity, dissolved organic matter and pollution. In other words, the term "turbidity" refers to the material that is transported in suspension by the water. Turbidity distribution patterns on satellite images help in monitoring distribution and movement of turbid water masses (KUNTE, 1994). Indeed, coastal currents, water circulation and the modifying influence of wind on water circulation can be detected by examining the spatial and temporal distribution patterns of suspended sediments (MURALIKRISHNA, 1980; KLEMAS and HARDISKY, 1987; FIEDLER and LAURS, 1990), where water circulation is deduced from the elongated patterns of turbidity plumes. Thus, a qualitative interpretation of the turbidity patterns within a dynamic perspective allows one to infer the general characteristics of the suspended sediment transport and the consequent horizontal movement of the surface waters.

Fig. 1. The study area is situated in the Atlantic coast of Buenos Aires province (Argentina) and in the southern portion of Anegada bay. San Blas channel, with a SE-NW orientation, is the southern tidal inlet that connects the bay with the continental shelf.

As turbidity increases, the reflectance from the water is enhanced. This parameter, detectable by Landsat reflective bands, has been extensively used as a natural tracer of water circulation patterns (BABAN, 1994, 1995; CHICA-OLMO et al., 2004; KUNTE, 1994; OJEDA et al., 1995; PATTIARATCHI et al., 1986; ULIBARRENA and WEBER, 2007). KUNTE (1994) determined the shore-drift direction along the Kerala coast (India) by studying the shape of the turbidity plumes observed in Landsat images. Similarly, using a Landsat 5 image, BABAN (1995) deduced the water circulation patterns adjacent to the mouth of the river Yare (Norfolk) from the elongated shapes of sediment plumes. The water circulation patterns as well as the sediment plumes are believed to be a function of the fluvial discharge into the North Sea, the tide and the speed and direction of the wind (BABAN, 1995). The water dynamics along the Mar del Plata coast and adjacent areas (Argentina) have also been analyzed using aerial photographs and satellite images (Spot, Landsat, Quickbird) (ULIBARRENA and WEBER, 2007). Flow patterns in the vicinity of an offshore sandbank (the Scarweather Sands, northern Bristol Channel) during a tidal cycle were identified by PATTIARATCHI et al. (1986) using suspended sediments detected by remotely sensed imagery (Airborne Thematic Mapper) as passive tracers. The results showed good correlation with surface vector current measurements, predicted tidal currents and field observations made at the times of the aircraft´s overpasses (PATTIARATCHI et al., 1986).

Analyzing turbidity patterns in 12 Landsat TM and Spot HRV images associated with different hydrodynamic conditions in the Tinto – Odiel estuary (SW Spain), OJEDA et al. (1995) studied the water circulation in the estuary during a theoretical tidal cycle. The qualitative interpretation of the turbidity patterns allowed them to characterize the main aspects of the estuarine dynamics (tidal currents, turbidity maximum, coastal and estuarine water mixing processes) and determine flow schemes in the estuary mouth (OJEDA et al., 1995). These dynamic studies in the Tinto-Odiel estuary system were continued by CHICA-OLMO et al. (2004), who applied Principal Component Analysis (PCA) to a set of Landsat images in order to identify turbidity levels and flow directions during average high to low tides.

In a similar way, in this paper we try to understand the development of the bedforms at both ends of the channel analysing the turbidity and water circulation patterns in the San Blas channel during a theoretical tidal cycle. For this purpose, a set of 8 Landsat TM and ETM images of the study area were analyzed. Although the Landsat visible channels do not penetrate far into the turbid water (LATHROP and LILLESAND, 1989), thus reducing the utility of turbidity patterns in dynamic studies to surface waters (OJEDA et al., 1995), the well-mixed San Blas channel, characterized by prevailing homothermal and homohaline vertical profiles and intense tidal currents (ALVAREZ and RÍOS, 1983), is considered an appropriate environment for the application of this approach.

Study Area

The channel (13-km long) has a SE-NW orientation with a mean width of 2 km and an average depth of 27 m. Winds and tides are the main forcing agents that influence the water circulation in the study area. The channel is affected by a mixed tidal regime with a semidiurnal predominance. Average tidal heights are 0.57 m (low tide) and 2.21 m (high tide) (SHN, 2009). Winds from the South Atlantic (warm, humid air) and South Pacific (cold, dry air) semipermanent high-pressure systems dominate the regional atmospheric circulation. From December 2007 to December 2008, a meteorological station was installed on the San Blas channel coast. These data showed prevailing and stronger winds from the NE quadrant, which usually cause time delays with respect to the predicted tides in the San Blas channel (BEIGT et al., 2009).

Only a few studies have focused on the hydrodynamics of the San Blas channel (ALVAREZ and RÍOS, 1983; ALVAREZ et al., 2009a, b; CUADRADO and GÓMEZ, 2010b). During 13 oceanographic campaigns (June 1980- August 1982), ALVAREZ and RÍOS (1983) registered water temperature, salinity, and current intensity at various stations along the channel. They found average temperatures of 20ºC and 7,8ºC in summer and winter, respectively, and horizontal thermal gradients of 0.5 – 1.6ºC km^{-1}, reaching 2.2 and 9.5ºC km^{-1} in winter, near the southwestern coast of Gama island (Fig. 1). An area of thermal differences was located at the south of Gama island, where a sharp change in water color was observed during ebb tide, indicating suspended sediment transport. The authors suggest the possible occurrence of small-scale circulation patterns in the internal area of the channel (ALVAREZ and RÍOS, 1983). They found prevailing homothermal and homohaline vertical profiles, indicating that tidal currents are strong. Maximum current intensities reaching 206 cm s^{-1} (measured at mid-depth) were recorded near the channel mouth, decreasing towards the internal area of the channel (78 – 86 cm s^{-1}). In the external zone seaward of the channel mouth, they found current velocities of 65 – 82 cm s^{-1}. ADCP velocity profiles measured recently across San Blas channel showed maximum values of 200 cm s^{-1} during flood tide and 180 cm s^{-1} during ebb tide (CUADRADO and GÓMEZ, 2010a,b). ALVAREZ et

al. (2009a) and CUADRADO and GÓMEZ (2010b) found that flood currents are more intense from the surface to 10m depth on the northeastern coast, while ebb currents show maximum intensities from the surface to 18m depth on the southwestern coast. Preliminary results of a numerical model of the tidal circulation in San Blas channel are qualitatively coincident with these ADCP results (ALVAREZ et al., 2009b).

Geological and Morphological Settings

Different authors have performed sedimentological (CORTELEZZI et al., 1968; CORTELEZZI AND DILLON, 1974; TERUGGI et al., 1962), geological and morphological (AMBROSINI, 1984; FRENGUELLI, 1950; GONZÁLEZ et al., 1986; NICOLÁS et al., 1986; TREBINO, 1986; WEILER, 1988, 1993, 1998; WITTE, 1916) studies in the area of San Blas and Anegada bay. Particularly, the geomorphology of Jabalí island (off the southwestern coast of the San Blas channel) (Fig. 1) and adjacent areas has been described in detail by AMBROSINI (1984) and TREBINO (1986). The Quaternary sedimentary cover is composed of marine and continental deposits. Pleistocene deposits include: sandy gravel deposits from an old alluvial plain ("*rodados patagónicos*"), edaphized sand deposits from old dunes, and *rodados patagónicos* and gravel deposits from Pleistocene littoral ridges. Holocene deposits include: *rodados patagónicos* and gravel deposits from littoral ridges, salt pan deposits, beach and dune sand deposits, and silty clay deposits from tidal flats and tidal channels (Jabalí and Del Guanaco creeks, Fig. 1) (TREBINO, 1986). Both authors draw a distinction between the northern coast of the island (characterized by a narrow and steep gravel beach) and the southern coast (southward from Baliza La Ballena, Fig. 1) with a wide, medium to fine-grained sandy beach. The former was identified by TREBINO (1986) as an erosional coast with active cliffs of varying heights (0.80 - 5m) cut into littoral ridge deposits, while the latter was described as an accretional coast with a gentle slope gradient. A transitional area extends from La Rebeca to Baliza La Ballena (Fig. 1). Northward from Punta Ramirez, CUADRADO and GÓMEZ (2010a) identified salt marshes and abrasion platforms.

The subaqueous morphology of the San Blas channel was studied by ALVAREZ and RÍOS (1983) and recently by CUADRADO and GÓMEZ (2010a,b). ALVAREZ and RÍOS (1983) identified a dune field in the central portion of the channel and a flat to slightly undulated bottom along the southwestern end of the channel by bathymetric tracks. A detailed bathymetry and a morphological map of the channel have recently been obtained by CUADRADO and GÓMEZ (2010a,b) using a Phase Measuring Bathymetric Sonar System (Geoswath Bathymetry System Plus, GeoAcoustic Ltd.). Based on the subaqueous morphology and tidal current measurements, they defined the channel as a "tidal inlet throat" and identified ebb and flood-tidal deltas at both ends of the channel (Fig. 2), which are typical morphological features of a tidal inlet (DAVIS and FITZGERALD, 2004). Moreover, they described a sand dune field located at the inner end of the inlet throat, at an average depth of 22 m. Based on the differential migration of these subaqueous dunes, the authors proposed a circulation model for sand transport in San Blas channel. They found that very large dunes (4.5 – 5 m height) situated near the southwestern limit of the dune field migrate towards the channel mouth at an average migration rate of 37.5 m year^{-1}. Large dunes (2 - 2.5 m height) on the northern flank migrate in the opposite direction, towards Anegada bay (average migration rate of 27 m year^{-1}) (CUADRADO and GÓMEZ, 2010b). The inlet throat shows the maximum depths (28 m) and a U-shaped transversal channel profile, free of unconsolidated sediment.

METHODS

Eight Landsat TM and ETM images acquired under clear-sky conditions and representing different tidal stages were selected from a pool of Landsat images provided by CONAE (Argentinian National Commission of Space Activities) and the US Geological Survey, through its Earth Resources Observation and Science (EROS) data center. Average wind speed and direction on satellite overpass dates were estimated by means of the regional LAHM/CIMA model (COMPETELLA and SAULO, 2003) from the CIMA (Argentinian Research Center of the Sea and the Atmosphere).

Standard digital image processing techniques within Erdas Imagine 9.1 were used to perform geometric and radiometric corrections on the visible (1-3) and near-infrared (4) bands (APN-SIB, 2005). Image-to-image registration was performed using a geometrically corrected Level1T USGS Landsat image. At-satellite spectral radiance (L_{sat}) was obtained by calibration (1):

$$L_{sat} = G \cdot DN + B \quad (1)$$

where G and B are the gain ((W m^{-2} sr^{-1} mm^{-1})/DN) and bias (W m^{-2} sr^{-1} mm^{-1}) calibration coefficients for the given spectral band, respectively, and DN is the pixel digital number.

Calibration coefficients were extracted from CHANDER et al. (2009). An image-based atmospheric correction (COST method by CHAVEZ (1996)) was applied (2):

$$\rho = \frac{\pi \left(L_{sat} - L_{haze}\right)}{T_v \left(E_0 \cdot \left(\cos\left(\theta_z\right)\right)^2 + E_{down}\right)} \quad (2)$$

where r is the surface reflectance; L_{haze} is the path radiance (W m^{-2} sr^{-1} mm^{-1}); T_v is the atmospheric transmittance from the ground surface to the sensor; E_0 is the exoatmospheric solar constant (W m^{-2} mm^{-1}); θ_z is the solar zenith angle and E_{down} is the downwelling diffuse irradiance (W m^{-2} mm^{-1}).

CHAVEZ (1996) assumes that T_v = 1.0 and E_{down} = 0.0 (i.e., ignores downwelling). The COST method and the previous Dark-object subtraction (DOS) technique by CHAVEZ (1988) have been extensively applied in similar turbidity studies reported in the literature (see e.g. BABAN (1997), KABBARA et al. (2008), MILLER et al. (2005)).

The path radiance was estimated as (SONG et al., 2001) (3):

$$L_{haze} = G \cdot DN_{haze} + B - (0.01 / \pi) \quad (E_0 \cdot (\cos(\theta_z))^2 \tag{3}$$

where DN_{haze} is the dark-object digital number.

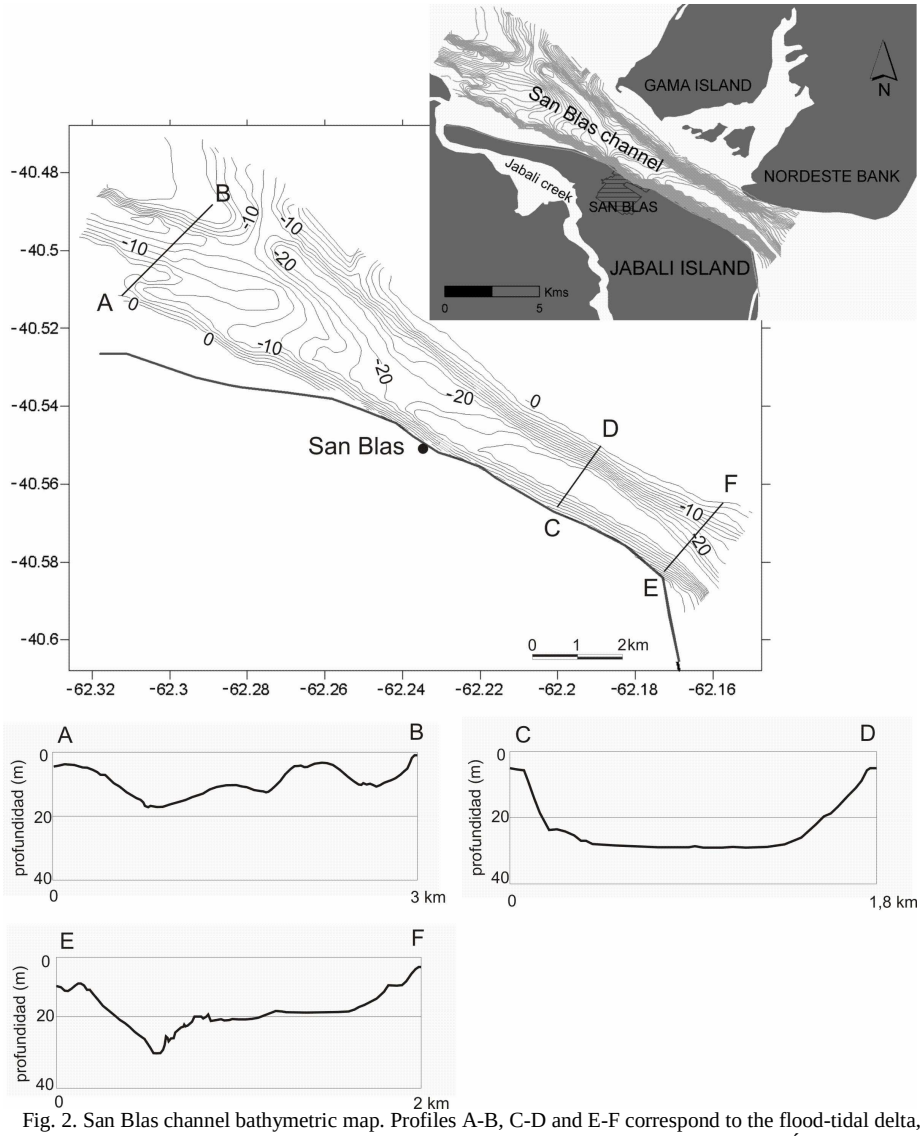

Fig. 2. San Blas channel bathymetric map. Profiles A-B, C-D and E-F correspond to the flood-tidal delta, the tidal inlet throat and the ebb-tidal delta, respectively (modified from CUADRADO and GÓMEZ, 2010b).

DN_{haze} values were selected by looking at areas of known zero reflectance in the near-infrared band (i.e. deep Atlantic ocean water within the coverage of the Landsat scene, path: 226, row: 88) (Fig. 3) and assuming that any value other than zero in the raw image in these areas represents haze effect (MAHINY and TURNER, 2007). Continental areas, islands and breaking waves were masked out and an ISODATA unsupervised classification was performed. TM3 and ETM3 bands were chosen for this study for various reasons: a) the red portion of the visible spectrum is less sensitive to the influence of bathymetry than the shorter wavelength bands (HERNÁNDEZ BARTOLOMÉ and HERNÁNDEZ CALVENTO, 2003; OJEDA et al., 1995) due to its less penetrative power (BABAN, 1995); b) suspended sediments increase backscattering in the longer wavelength portion of the visible spectrum (TOOLE and SIEGEL, 2001; MILLER ET AL., 2005) and c) these bands were identified as those that better discriminate turbidity levels in the study area.

Results and Discussion

The Landsat images were classified into 3 classes or turbidity levels (low, medium and high) and separated into 2 groups (ebb/flood tide) depending on the tidal stage (Fig. 4A to H). A qualitative interpretation of the turbidity patterns in the San Blas channel from a dynamic perspective allow us to infer the general characteristics of the suspended sediment transport along the channel and the consequent horizontal movement of the surface waters during a theoretical tidal cycle. High turbidity levels during ebb tide (Fig. 4A to C) are mainly observed in the internal area of Anegada bay and at the seaward end of the channel. At mid-tide conditions during ebb tide, the turbidity shows maximum values on both channel flanks (Fig. 4B), indicating a high suspended sediment transport. Taking into account that medium to fine-grained sand covers the channel bed (CUADRADO and GÓMEZ, 2010b), strong currents must carry and/or resuspend these sediments at shallower depths. At the seaward end of the channel, ebb currents feed the ebb-tidal delta flowing in a wide-spread direction into the open sea and curving clockwise to the south. During flood tide (Fig. 4D to H), the high turbidity zone is the inner area of Anegada bay, where a flood-tidal delta is present. This is probably related to the effect of bottom resuspension at these shallower depths. The flood currents enter the channel following

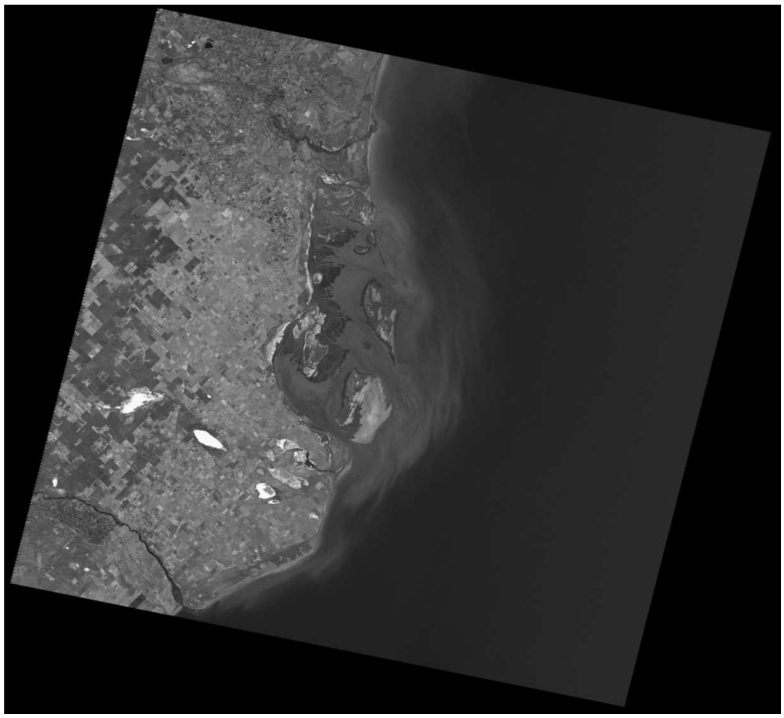

Fig. 3. Landsat scene (ETM3 band, 226/ 88).

the pathways of the ebb tidal delta channels (Fig. 5B) and suspended sediment transport occurs mainly along the southern coast of the channel. The southern coast of Jabalí island (southwestern portion of the ebb-tidal delta, Fig. 5) is an area of high turbidity levels during flood tide as well as during ebb tide (Fig. 4). This is interpreted as a result of the littoral drift in this area, which comes from S to N along the Buenos Aires coast (SCHNACK et al., 1982).

Estimated wind speed and direction on satellite overpass dates are also shown in Figure 4. The strong SW wind in Fig. 4A is opposed to the ebb currents direction in the inner NE area of Anegada bay, probably creating an increase in the water height that is observed in the classified image as an area of low-to-medium surface turbidity (indicated by an ellipse in Fig. 4A). The same situation is generated in nearly low tide conditions (Fig. 4C) with a SW wind of 64 km/h. Conversely, in calm conditions (Figs. 4E and F) as well as with a NW wind opposed to the flood currents (Fig. 4G), the depths are shallower and the bottom sediment resuspension and suspended sediment are observed throughout the whole inner bay.

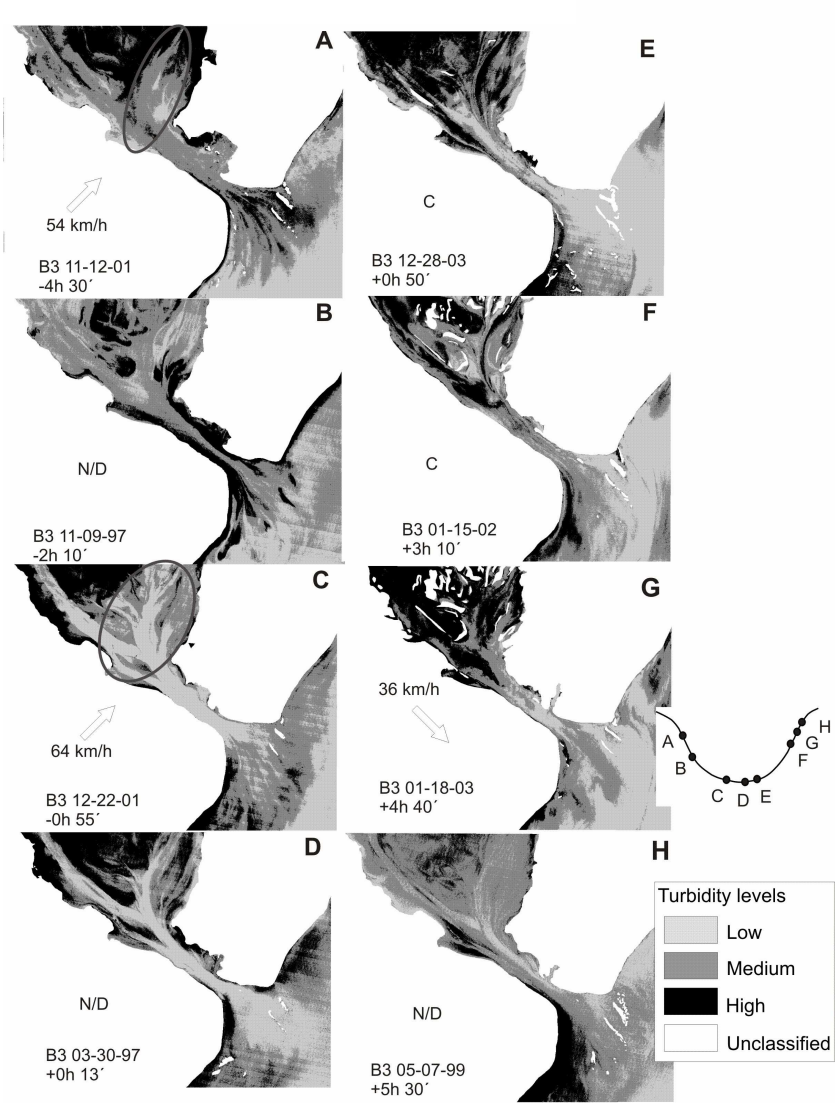

Fig. 4. ISODATA classification of TM3 and ETM3 bands showing turbidity ranges during a theoretical tidal cycle. Time to (-) and from (+) low tide. Average wind direction is indicated by arrows (C = calm conditions; N/D = no data). Wind speed is shown beside the arrows. A) to C): Ebb tide; D) to H): Flood tide.

The turbidity patterns observed in the Landsat images have a close relation to the morphological features of the channel bed described by CUADRADO and GÓMEZ (2010b) (i.e., the tidal inlet throat and the tidal deltas). The narrow (900 m), deep (28 m) tidal inlet throat (Fig. 2) is a highly dynamic area where the current velocity increases, removing all the unconsolidated sand sediments and leaving an area completely sediment-free. This is shown in figure 4, where the deepest area of the tidal inlet throat is relatively free of suspended sediments, with a low-to-medium turbidity level throughout the tidal cycle. Only the shallower flanks are affected by a high turbidity level and suspended sediment transport (e.g. Fig. 4B). Minimum turbidity levels throughout the San Blas channel are observed under nearly low tide conditions (Fig. 4C and D). At both ends of the channel, the sediment deposition caused by the reduction in the carrying capacity leads to the formation of an ebb and a flood tidal deltas (CUADRADO and GÓMEZ, 2010b). Both areas (Fig. 5) generally show a high turbidity (Fig. 4) due to shallower depths.

From the elongated shape of the turbidity plumes, general tidal circulation patterns were identified in the San Blas channel (Fig. 6): a) ebb currents run in different directions across the flood-tidal delta, b) seaward from the channel mouth, these currents flow in a wide-spread direction into the open sea, curving towards the south, c) the flood currents coming from the SW follow the pathways of the ebb tidal delta channels, d) in the internal area of Anegada bay, the flood currents run in different directions across the flood-tidal delta.

In summary (Fig. 7), ebb currents running in different directions across the flood-tidal delta trigger turbidity along both channel flanks. These currents carry suspended sediment in a wide-spread direction into the open sea, curving towards the south, generating the ebb tidal delta. Prevailing and stronger winds from the NE quadrant (BEIGT et al., 2009) probably generate local waves that affect the geometry of the ebb tidal delta, which tends to rotate in a clockwise direction (Fig. 5b). The delta (especially those banks that are curved clockwise towards the south) is also reworked by flood currents (Fig. 6b). The direction of these currents in this area is nearly SW-NE due to the tidal wave coming from the south (ALVAREZ and RÍOS, 1983). These currents enter the channel follo wing the pathways of the ebb tidal

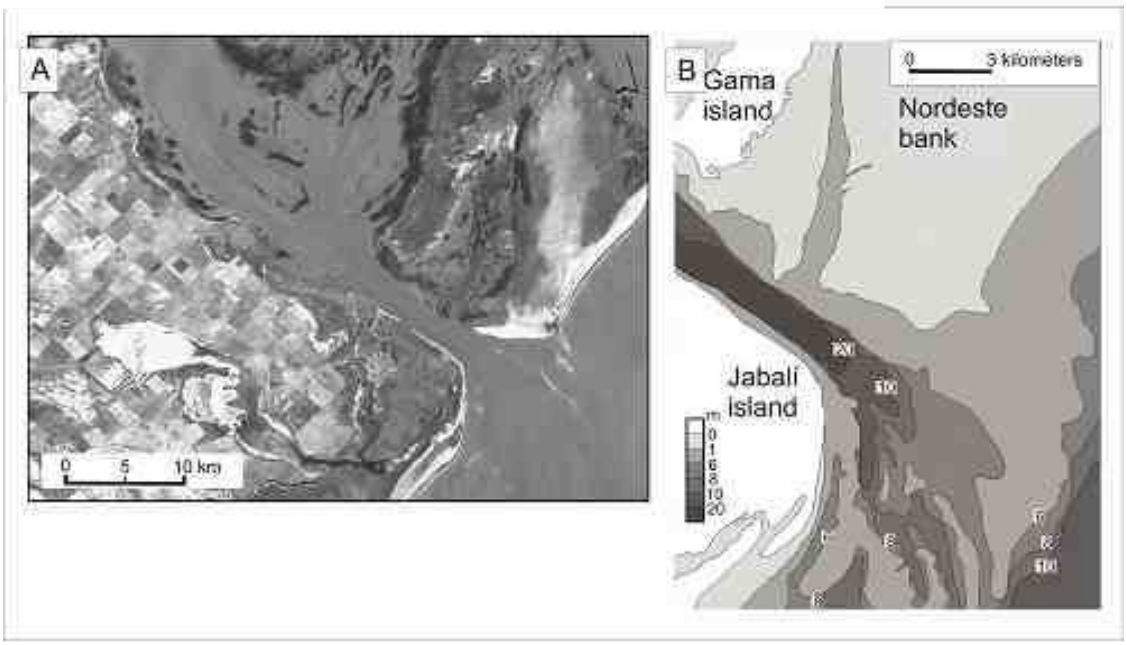

Fig. 5. **A)** Flood and ebb-tidal banks observed in a Landsat 7 image (01-15-02). **B)** Nautical chart (SHN, 1972) showing the submarine banks curved in a clockwise direction toward the south.

delta channels (Fig. 5B). In the inner channel, flood currents transport suspended sediment mainly along the southern coast, generating a flood-tidal delta with elongated banks extending in the direction of the tidal currents, which run along four main branches among the delta banks (Fig. 7b). Finally, the littoral drift coming from S to N in the external area seaward from the channel mouth, generates the sediment transport and/or resuspension on the banks that are closer to the shore. This is observed during both ebb and flood tide.

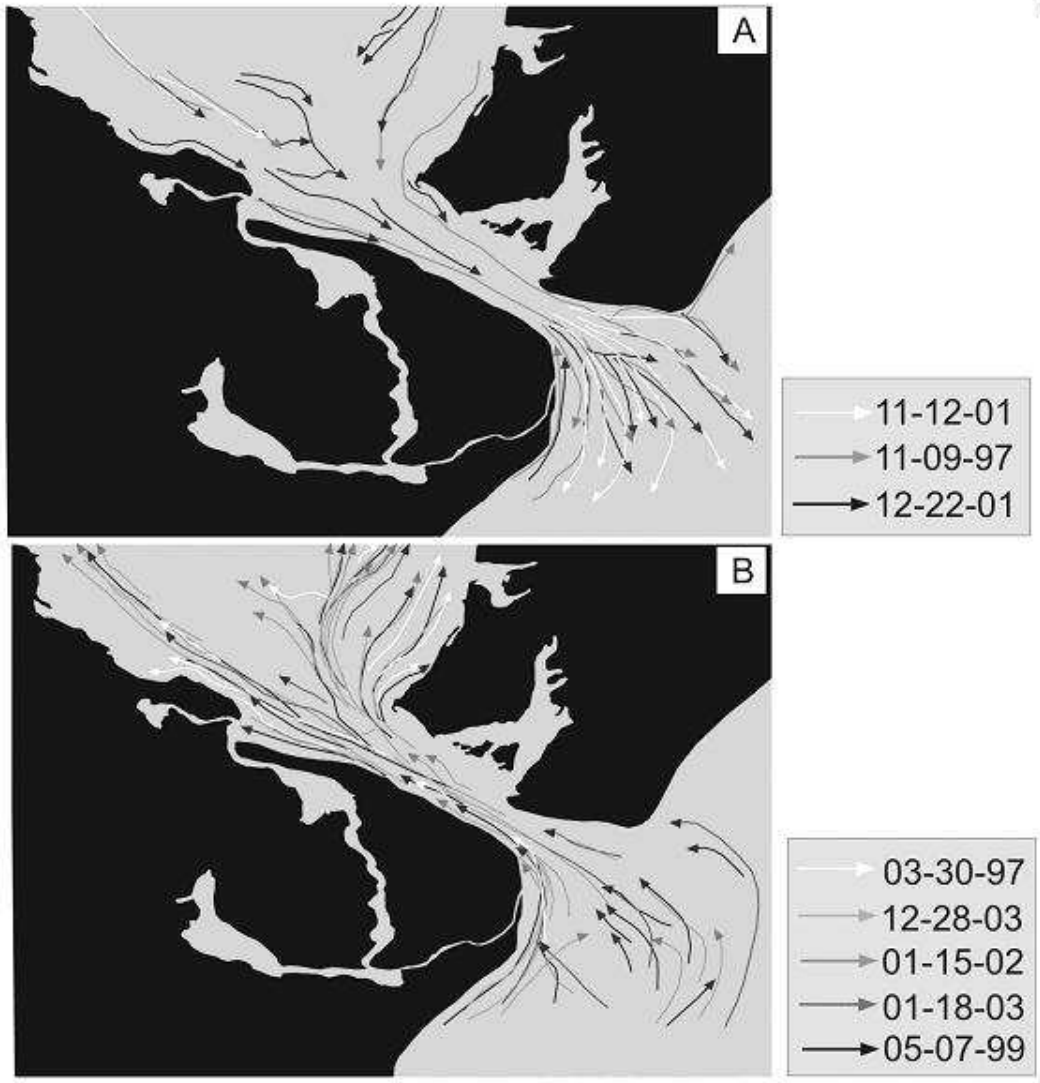

Fig. 6. Turbidity plumes showing the flow directions during the satellite overpasses. **A)** ebb tide, **B)** flood tide.

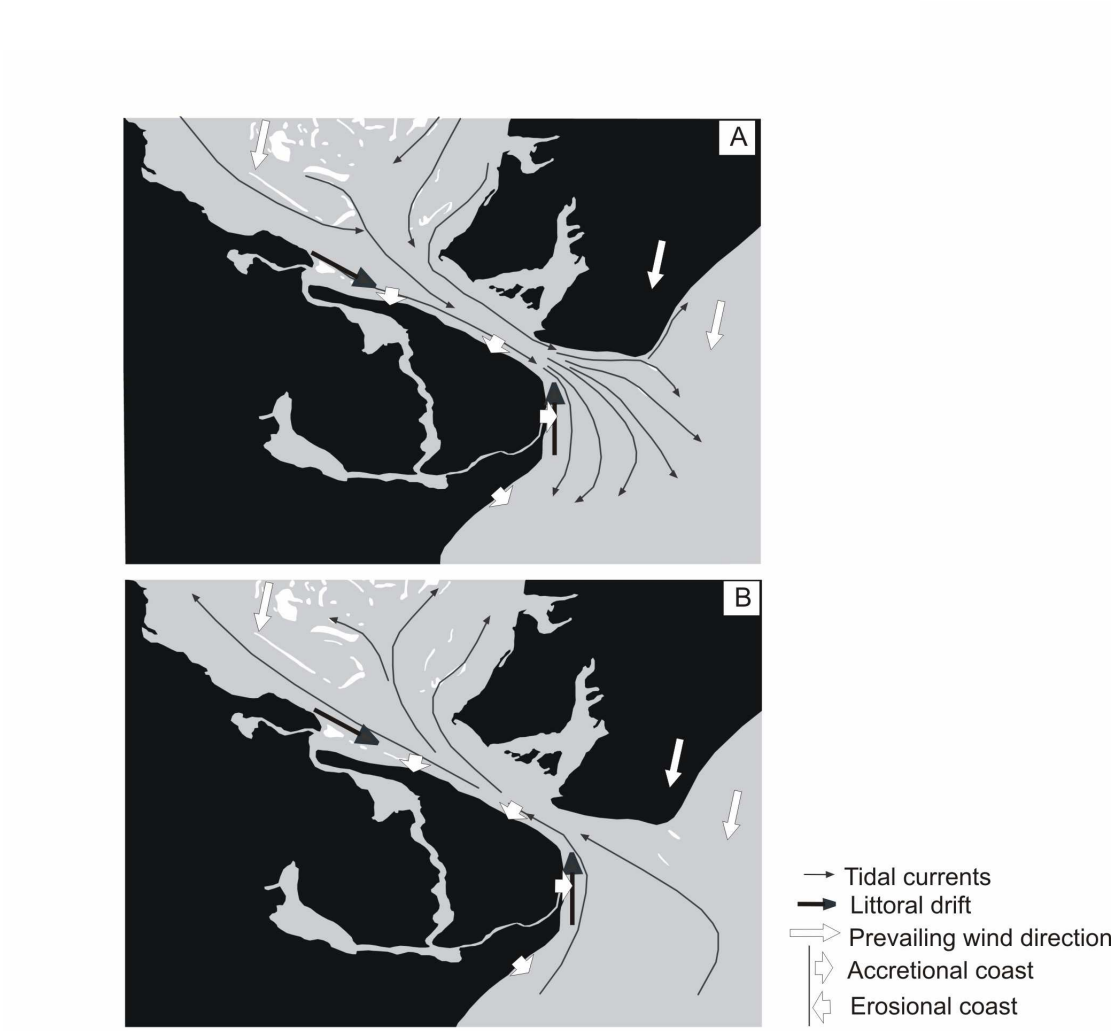

Fig. 7. Main flow directions during **A)** ebb tide and **B)** flood tide. Prevailing wind direction (BEIGT et al., 2009), littoral drift directions and accretional/erosional coasts (TREBINO, 1986) are indicated by arrows. The tidal deltas and the modern spit observed in satellite images are shown in white.

Accretional areas along the southwestern coast of the channel may be inferred from the turbidity patterns. From Baliza La Ballena (Fig. 1) to the south, the accretional coast identified by TREBINO (1986) is an area of high turbidity during flood tide as well as during ebb tide. As mentioned previously, this is interpreted as a result of the S-N littoral drift. Another accretional area is located in front of Jabalí creek mouth, where a modern spit (Fig. 7) is growing in the longshore drift direction along the channel, towards the channel mouth. Similarly, this area generally shows a high turbidity (Fig. 4), indicating high suspended sediment concentrations over the spit.

The circulation model for sand transport along the San Blas channel proposed by CUADRADO and GÓMEZ (2010b) (based on the differential migration of the subaqueous dunes from a sand dune field located at the inner end of the channel) can be completed with the results shown here referred to the surface water circulation. The mentioned model indicates a bottom sediment transport towards the inner Anegada bay area along the northern flank of the channel. Conversely, sand transport by ebb currents occurs in the opposite direction along the southern flank. The results shown here suggest that suspended sediment transport towards the channel mouth by ebb currents occurs along both flanks, while flood currents trigger turbidity mostly over the southern flank of the channel (Fig. 7).

Conclusions

As mentioned in the introduction, only a few previous studies have focused on the hydrodynamics of the San Blas channel. In an attempt to partially fill the knowledge gap regarding the water circulation in the San Blas channel, this investigation studied the suspended sediment transport as well as the horizontal movement of the surface waters during a theoretical tidal cycle in the channel, using turbidity detected by Landsat reflective bands as a natural tracer. The use of satellite imagery allowed us to obtain a synoptic view of the turbidity plumes according to tidal stage. The results suggest that an ebb-tidal delta is being developed seawards from the channel mouth, as a result of: a) the ebb currents that carry sediment along both flanks and in a wide-spread direction into the open sea, b) the local waves generated by prevailing NE quadrant winds, which force the delta to rotate in a clockwise direction, c) the flood currents that rework the delta, especially those banks that are curved towards the south and d) the sediment transport and/or resuspension by the S-N longshore drift in the banks that are closer to the coast of Jabalí island. In the inner Anegada bay, a flood-tidal delta with elongated banks in the direction of the tidal currents is being generated by flood currents, which trigger turbidity mostly along the southern flank of the channel and then run in four main directions across the flood-tidal delta. This delta is also reworked by ebb currents running across the delta in similar directions as the flood currents.

Acknowledgements

The authors wish to thank Oc. Eder Paulo Dos Santos for his help with the Portuguese translation of the abstract. This study was financially supported by a post-doctoral research grant awarded by CONICET (National Council for Scientific and Technological Research) (Res. N° 0028/08) and by the National Agency for Scientific and Technological Promotion, ANPCyT (PAE 22666/04) and the Secretariat for Science and Technology, SeCyT-UNS (PGI 24/ZH15).

References

ALVAREZ, L. I.; ALBERDI, E.; CUADRADO, D. G.; PERILLO, G. M. E. Caracterización de la hidrodinámica del canal de San Blas mediante la utilización de un ADCP. **Resúmenes de las VII Jornadas Nacionales de Ciencias del Mar, Bahía Blanca (in CD-ROM).** 2009a.

ALVAREZ, L. I.; ALBERDI, E.; CUADRADO, D. G.; PERILLO, G. M. E. Modelo numérico preliminar de la circulación de la corriente en Bahía San Blas. **Resúmenes de las VII Jornadas Nacionales de Ciencias del Mar, Bahía Blanca (in CD-ROM).** 2009b.

ALVAREZ, J. A.; RÍOS, F. F. Estudios litorales en las bahías de San Blas y San Antonio Oeste. Caracterización oceanográfica preliminar de la zona interior de la Bahía San Blas, provincia de Buenos Aires.. 39 pp. **Actas del VIII Simposio Latinoamericano de Oceanografía Biológica, Montevideo.** 1983

AMBROSINI, G. L. Geomorfología de la Isla del Jabalí, Departamento de Patagones, provincia de Buenos Aires. **Actas III del IX Congreso Geológico Argentino, San Carlos de Bariloche**. p. 497–512. 1984.

APN (Administración de Parques Nacionales) – SIB (Sistema de Información de Biodiversidad). **Protocolo para el preprocesamiento de imágenes satelitales Landsat para aplicaciones de la Administración de Parques Nacionales.** 2005. 21 pp. Buenos Aires. http://www.sib.gov.ar/archivos/Protocolo_img_Landsat.pdf

BABAN, S. M. J. Mapping turbidity, surface temperature and water circulation patterns with the aid of satellite imagery. J. Inst. **Water Environ. Management**, n. 8, p. 197–204, 1994.

BABAN, S. M. J. The use of Landsat imagery to map fluvial sediment discharge into coastal waters. **Mar. Geol**., n. 123, p. 263 – 270, 1995.

BABAN, S. M. J. Environmental monitoring of estuaries; estimating and mapping various environmental indicators in Breydon Water Estuary, U.K., using Landsat TM imagery. **Estuarine, Coastal and Shelf Science**, n. 44, p. 589-598, 1997.

BEIGT, D.; CUADRADO, D. G.; PICCOLO, M. C. Resultados preliminares del efecto del viento en la marea de Bahia San Blas. 2009. p. 287-288. **Actas de la XXIV Reunión Científica de la Asociación Argentina de Geofisicos y Geodestas**, Mendoza, Argentina.

CHANDER, G.; MARKHAM, B. L.; HELDER, D. L. Summary of current radiometric calibration coefficients for Landsat MSS, TM, ETM+ and EO-1 ALI sensors. **Remote Sens. Environ**., n. 113, p. 893–903, 2009.

CHAVEZ, P. S. An improved dark-object subtraction technique for atmospheric scattering correction of multispectral data. **Remote Sens. Environ**., n. 24, p. 459–479, 1988.

CHAVEZ, P. S. Image-based atmospheric corrections – Revisited and improved. Photogramm. **Eng. Rem. S.,** v. 62, n. 9, p. 1025–1036, 1996.

CHICA-OLMO, M.; RODRIGUEZ, F.; ABARCA, F.; RIGOL-SANCHEZ, J. P.; DEMIGUEL, E.; GOMEZ, J. A.; FERNÁNDEZ-PALACIOS, A. Integrated remote sensing and GIS techniques for biogeochemical characterization of the Tinto-Odiel estuary system, SW Spain. **Environ. Geol**., n. 45, p. 834–842, 2004.

COMPETELLA, C.; SAULO, C. Verificación objetiva del modelo LAHM/CIMA sobre el centro-este de Argentina y Uruguay. **Meteorológica**, v. 28, n. 12, p. 83–96, 2003.

CORTELEZZI, C. R.; DE SALVO, O.; DE FRANCESCO, F. Estudio de las gravas tehuelches de la región comprendida entre el río Negro y el río Colorado desde la costa atlántica hasta la cordillera. **Actas III de las II Jornadas Geológicas Argentinas, Buenos Aires**. p. 123–141. 1968.

CORTELEZZI, C. R.; DILLON, A. Estudio de las variaciones morfológicas en las playas de la zona de San Blas, partido de Patagones, provincia de Buenos Aires. **LEMIT** An., n. 2, p. 75–84, 1974.

CUADRADO, D. G.; GÓMEZ, E. A. Geomorfología y dinámica del canal San Blas, Provincia de Buenos Aires (Argentina). **Lat. Am. J. Sedimentol. Basin Anal**., v. 17, n. 1, p. 3-16, 2010a.

CUADRADO, D. G.; GÓMEZ, E. A. Circulación sedimentaria en una garganta de marea de la costa argentina. **LAJAR**, in press, 2010b.

DAVIS JR., R. A.; FITZGERALD, D. M. **Beaches and Coasts.** United Kingdom: Blackwell Science Ltd, 2004. 405 pp.

FIEDLER, P. C.; LAURS, R. M. Variability of the Columbia River plume observed in visible and infrared satellite imagery. **Int. J. Remote Sensing**, v. 11, n. 6, p. 999–1010, 1990.

FRENGUELLI, J. **Rasgos generales de la morfología y la geología de la provincia de Buenos Aires**. Ministerio de Obras Públicas, Provincia de Buenos Aires, Serie II, n. 33, p. 14–20, 1950.

GONZÁLEZ, M. A.; WEILER, N. E.; GUIDA, N. G. Late Pleistocene transgressive deposits from 33º S.L. to 40ºS.L., Argentine Republic. **J. Coastal Res., Special Issue** n. 1, p. 39–48, 1986.

HERNÁNDEZ BARTOLOMÉ, J. F.; HERNÁNDEZ CALVENTO, L. Aplicación de técnicas de teledetección al estudio de la turbidez de las aguas litorales en la costa oriental de Gran Canaria mediante un modelo teórico. **Vegueta,** n. 7, p. 229–240, 2003.

KABBARA, N.; BENKHELIL, J.; AWAD, M.; BARALE, V. Monitoring water quality in the coastal area of Tripoli (Lebanon) using high-resolution satellite data**. ISPRS J. Photogramm.,** n. 63, p. 488–495, 2008.

KLEMAS, V.; HARDISKY, M. A. Remote sensing of estuaries: an overview. 1987. pp 183 – 204. **Symp. Remote Sensing of Environment,** Ann Arbour, Michigan.

KUNTE, P. D. Potential usage of remote sensing data in studying the behaviour of shore drift along Kerala Coast, India. **Estuar. Coast. Shelf S.,** n. 38, p. 613-624, 1994.

LATHROP, R. G.; LILLESAND, T. M. Monitoring water quality and river plume transport in Green Bay, Lake Michigan, with SPOT-1 imagery. **Photogramm. Eng. Rem. S.,** n. 55, p. 349–354, 1989.

MAHINY, A. S.; TURNER, B. J. A comparison of four common atmospheric correction methods. **Photogramm. Eng. Rem.** S., v. 73, n. 4, p. 361–368, 2007.

MILLER, R. L.; MCKEE, B. A.; D´SA, E. J. Monitoring bottom sediment resuspension and suspended sediments in shallow coastal waters. In: Miller, R. L., Del Castillo, C. E., McKee, B. A. (eds.). **Remote Sensing of Coastal Aquatic Environments.** Dordrecht: Springer, 2005. p. 259–276.

MURALIKRISHNA, I. V. Landsat application to the study of coastal processes. In: Salomnson, V.V. and Bhavsar, P.D. (eds.). The Contribution of Space Science to Water Resource Management (COSPAR Adv. Space Explor., g.). Oxford: **Pergamon,** 1980. 280pp.

NICOLÁS, R.; KOSTADINOFF, J.; SCHILLIZI, R. Correlación entre geoformas superficiales y observaciones geofísicas en la Bahía Anegada, provincia de Buenos Aires. **Rev. Asoc. Geol. Argent**., v. 41, n. 3-4, p. 245 – 255, 1986.

OJEDA, J.; SÁNCHEZ, E.; FERNÁNDEZ PALACIOS, A.; MOREIRA, J. M. Study of the dynamics of estuarine and coastal waters using remote sensing: The Tinto-Odiel estuary, SW Spain. **J. Coast. Conserv.,** v. 1, n. 1, p. 109–118, 1995.

PATTIARATCHI, C. B.; HAMMOND, T. M.; COLLINS, M. B. Mapping of tidal currents in the vicinity of an offshore sandbank using remotely sensed imagery. **Int. J. Remote Sens.,** n. 7, p. 1015–1029, 1986.

SCHNACK, E.; FASANO, J.; ISLA, F. The evolution of Mar Chiquita lagoon, Province of Buenos Aires, Argentina. In: Coloquhoum, D. (ed.), Holocene sea-level fluctuations: magnitudes and causes. University of South Carolina, Columbia, SC**.: IGCP Project 61**, 1982. p 143-155.

SHN (Servicio de Hidrografía Naval). **Carta Náutica**, H-260. 1972.

SHN (Servicio de Hidrografía Naval). **Tablas de marea**. Puertos de la República Argentina y algunos puertos de Brasil, Uruguay y Chile. Buenos Aires: Departamento de Artes Gráficas del SHN, 2009.

SONG, C.; WOODCOCK, C. E.; SETO, K. C.; LENNEY, M. P.; MACOMBER, S. A. Classification and change detection using Landsat TM data: when and how to correct atmospheric effects?. **Remote Sens. Environ., n**. 75, p. 230–244, 2001.

TERUGGI, M. E.; ETCHICHURY, M. C.; REMIRO, J. Las arenas de la costa atlántica de la Provincia de Buenos Aires, entre Bahía Blanca y Río Negro. **Actas II de las I Jornadas Geológicas Argentinas**, Buenos Aires. p. 351–358. 1962.

TOOLE, D. A.; SIEGEL, D. A. Modes and mechanisms of ocean colour variability in the Santa Barbara Channel. **J. Geophys. Res.-Oceans,** n. 106, p. 26985–27000, 2001.

TREBINO, L. G. Geomorfología y evolución de la costa en los alrededores del pueblo de San Blas, provincia de Buenos Aires. **Rev. Asoc. Geol. Argent**., v. 42, n. 1-2, p. 9–22, 1986.

ULIBARRENA, J.; WEBER, G. Análisis de la dinámica de las aguas costeras. In: Rivas, R.; Grisotto, A.; Sacido, M. Teledetección – **Herramienta para la gestión sostenible**. Buenos Aires: ed. Martín, 2007. p 559–565.

WEILER, N. E. Depósitos litorales del Pleistoceno Tardío y Holoceno en Bahía Anegada, provincia de Buenos Aires. 1988. p. 245–249**. Resúmenes de la II Reunión Argentina de Sedimentología,** Buenos Aires.

WEILER, N. E. Niveles marinos del Pleistoceno Tardío y Holoceno en Bahía Anegada, provincia de Buenos Aires: Geocronología y correlaciones. **Rev. Asoc. Geol. Argent.,** v. 48, n. 3-4, p. 207–216, 1993.

WEILER, N. E. Holocene sea levels in Anegada bay, Argentine Republic. **J. Coastal Res**., v. 14, n. 3, p. 1034–1043, 1998.

WITTE, L. Estudios geológicos de la región de San Blas. **Revista del Museo de La Plata,** tomo XXIV (2da. Serie Tomo XII, 1ra. parte), p. 1-99, 1916.

(Manuscript received 01 January 2010; revised 31 May 2011; accepted 05 June 2011)